Engineering a metabolomics workflow to capture single-cell diversity in 3D models

Hetzel, L.A.

Chapter IV

Resolving drug uptake heterogeneity in 3D organ on chip models via live single-ell microsampling and ion mobility mass spectrometry

Based on:

Vincent Verschoor*, Laura Castaneda*, Arnaud Nicolas, Bas Tretsch, Ahmed Ali, Thomas Hankemeier

Resolving drug uptake heterogeneity in 3D organ on chip models via live single-cell microsampling and ion mobility mass spectrometry

*Authors contributed equally

Manuscript under review

Abstract

Three-dimensional (3D) cancer cell models, such as spheroids, organoids, and organ-on-chip systems, provide more physiologically relevant conditions by preserving native cell–cell and cell–matrix interactions. However, analytical techniques that maintain and assess the intrinsic heterogeneity of these systems have lagged behind their biological complexity. Current approaches either rely on live imaging, which lacks biochemical depth, or destructive, high-content assays like RNA sequencing and mass spectrometry imaging, which require either fixative agents or freezing the 3D model before analysis. The key problem addressed here is the lack of methods that integrate live imaging with high-resolution biochemical analysis at the single-cell level.

We developed an integrated platform that bridges this gap by combining live imaging of a 3D cancer model with microsampling and mass spectrometry–based whole single-cell analysis. Using a vascularized organ-on-chip system cultured with HepG2 hepatocellular carcinoma cells under a drug gradient, we demonstrated the platform's ability to capture heterogeneous uptake of the drug Tamoxifen. By modifying a commercial organ-on-a-chip platform for precise microsampling, introducing a single-cell preparation technique to mitigate matrix interference from Matrigel, and incorporating High-field Asymmetric Waveform Ion Mobility Spectrometry (FAIMS), we reduced matrix contamination and enhanced signal-to-noise ratios. This workflow enables non-destructive linkage between dynamic imaging data and single-cell biochemical profiles, preserving the spatial and temporal integrity of 3D tumor models.

This platform enables capillary-based single-cell isolation and metabolomic analysis of individual cells from live 3D tumor microenvironments, overcoming limitations of current imaging and molecular methods. By integrating live microscopy with sensitive single-cell mass spectrometry, it offers a new route to investigate cellular heterogeneity, drug distribution, and therapeutic responses in realistic cancer models, advancing translational and preclinical cancer research.

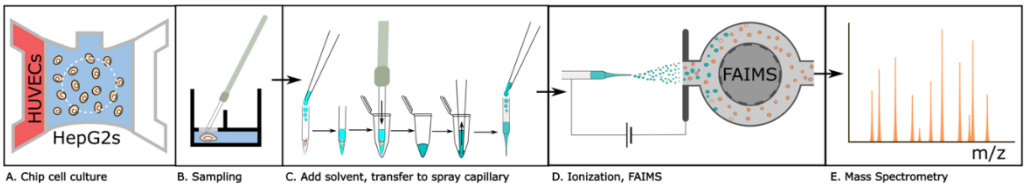

Introduction

Three dimensional (3D) cancer cellular models have emerged as superior disease models which represent *in vivo* physiological conditions better than traditional 2D models.[1,2] Models such as sandwiched models[3], spheroids,[4] organoids,[5] and organ-on-chip[6] preserve cell-cell interactions, as well as cellular interactions with the extra cellular matrix (ECM). However, as 3D models of cancer are further developed to retain the characteristics of the tumor microenvironment including the intrinsic physiological heterogeneity, the development of analytical techniques that are capable of measuring while preserving said heterogeneity has lagged behind. The need for such studies became more evident with the recent studies evaluating cancer drug resistance which identified hidden subtypes within the tumor with different DNA and protein expression.[7,8] Therefore, new techniques that possess the required single cell sensitivity and biochemical resolution are needed to fully map out the biochemical reactions in the tumor microenvironment in 3D models.

Current techniques that aim to elucidate the tumor microenvironment heterogeneity in 3D models are centered around live monitoring methods such as microscopy or methods which provide more chemical information of the tumor microenvironment at a static moment such as In-situ RNA sequencing and mass spectrometry imaging. Microscopic imaging of live single cells has minimal impact on the microenvironment, capturing the native cellular state[9], and revealing the interactions of different cell types influencing tumor progression.[10] This approach is suitable for observing cell behavior, however, it is limited in the biochemical information that can be gleaned from it. In an attempt to improve the biochemical information gained, fluorescence microscopy utilizes fluorescently tagged probes to attach to molecules of interest, e.g., proteins.[11,12] While this can provide more biochemical information at the single cell level, since the probes are specific

to a target molecule, the complete biochemical profile is still out of reach with just imaging techniques.[13] On the other end of the spectrum, technologies such as In-situ RNA sequencing and mass spectrometry imaging provide more biochemical information than imaging. However, they come with their own set of challenges.[14] Mainly, the extensive sample preparation that is required which typically includes cell fixation. This, in turn, disrupts the microenvironment and prevents repeated measurements. Consequently, the tumor microenvironment is evaluated as a static snapshot in biochemical terms, neglecting to account for its rapidly changing nature, which limits the extent of biological interpretation that can be gleaned from such techniques.[15] Raman spectroscopy has been used in 2D analyses; however, the limited penetration depth proves a debilitating obstacle for analysis in 3D applications.[16] Additionally, in 2D applications, Raman spectroscopy generates limited biochemical information compared to mass spectrometry.[16] In conclusion, analyzing the heterogeneity in the tumor microenvironment is limited to either highly dynamic microscopic imaging, with limited biochemical information, or trading the dynamic monitoring of the microenvironment in favor of more biochemical information via RNAseq. Therefore, further advances are needed in the field to be able to do both instead of choosing one or the other.

To achieve a better balance between dynamic monitoring and high biochemical information, integrated techniques can be used. For example, live microscopy can be used in combination with capillary Microsampling to both monitor the cell's environment and perform micro-sampling and biochemical assays with minimal disruption to said environment. In one approach a microscope is used to identify cells of interest and their surroundings. Then, target individual cells can be captured in a glass micropipette by applying negative pressure to a syringe connected to it.[17] The micropipette both acts as a sampling device, and a nano spray ionization source that introduces the contents of the pipette into the mass spectrometer for exhaustive biochemical analysis.[17] This method has been used successfully in 2D cell models to study drug uptake heterogeneity.[18] Another approach used a T-probe to capture the cell, introduce the ionization solvent and inject the sample into the mass spectrometer, enabling online

monitoring of single colon cancer cells.[19] The aforementioned methods showcases that live imaging can be combined with high biochemical methods such as mass spectrometry, but despite their promise, adapting such methods to 3D cell culture models remains a challenge. This is due to two key challenges. First, the ECM sampled with the single cells causes significant contamination and high noise in mass spectrometry measurements [20]. Second, the limited geometry of typical 3D platforms such as organ-on-chip models are incompatible with current capillary micro sampling techniques due to the relatively small inlets compared to the micro sampling capillary and angle of sampling. Specifically, for organ-on-chip platforms based on 384-well model microtiter plates, the angle required to reach the bottom of a well with a capillary is steep enough that the sampling capillary holder will block the path of light required for microscopic observation.

To address the aforementioned limitations, we developed the first integrated platform that is capable of both live monitoring of 3D cell models, as well as microsampling and mass spectrometry-based analysis of single-cells obtained from the 3D model with minimal disruption. To do this, we adapted a commercially available organ-on-a-chip model to allow for direct capillary sampling of whole single cells from a Matrigel environment. We then applied this platform to investigate the heterogeneity of cancer drug uptake in a hepatocellular carcinoma cell line cultured in a vascularized 3D organ-on-chip model where the drug was introduced from one vessel to form a 3D gradient. The cell line was specifically selected for the ability to uptake Tamoxifen, metabolize it into its active forms, and model the hepatotoxic effect.[21] The previous limitations such as the limited geometry and ECM effect on mass spectrometry measurements were circumvented by modifying a commercially available chip to allow for microsampling, incorporating a novel single-cell sample preparation technique to dilute the ECM, and using a High-field asymmetric-waveform ion-mobility spectrometry (FAIMS) to improve the signal to noise ratio of target molecules. This integrated platform will allow researchers, for the first time, to perform extensive single-cell analysis in complicated 3D tumor

microenvironment, while simultaneously monitoring said environment using advanced microscopy techniques.

Methods

HepG2 cell culture

Hepatocellular carcinoma cells (HepG2, HB-8065, ATCC) were maintained under standard cell culture conditions, 37°C, 5% CO_2, atmospheric O_2 levels, and ~90% relative humidity. Culture medium consisted of High Glucose Dulbecco's Modified Eagle Medium (DMEM) (D6546, Sigma-Aldrich), supplemented with 10% Fetal Calf Serum (FCS), 2 mM L-Glutamine (25030081, Thermo Fisher Scientific) and 1% penicillin/streptomycin (15070063, Thermo Fisher Scientific). Medium was refreshed every two to three days.

Cells were cultured in 100 mm TC-treated cell culture dishes (430167, Corning) and passaged at a ratio of 1:10 upon reaching 80% confluence. For passage, cells were released with 0.05% Trypsin/EDTA (15400054, Thermo Fisher Scientific) in Phosphate-Buffered Saline (PBS) for one minute in the incubator before adding complete medium to halt trypsin activity followed by pipetting to make a single cell suspension. Cells were passaged with a ratio of 1:10 by pelleting one tenth of the cell mixture for five minutes at 300 RCF and resuspending in complete medium before adding to a new cell culture dish.

For use in experiments, cells were used upon reaching 80% confluence and harvested as described above.

HUVEC cell culture

Human Umbilical Vein Endothelial Cells (HUVECs) were maintained under standard cell culture conditions, at 37°C, 5% CO_2, atmospheric O_2 levels and high humidity. Cell culture medium consisted of MV-2 Growth Medium (C-22121, PromoCell). Medium was refreshed every two to three days.

Cells were cultured in T75 flasks (50-809-261, Thermo Fisher Scientific) coated with Gelatin. To coat, 5 mL 2% Gelatin (G2500, Sigma-Aldrich) w/v solution in MilliQ water was added to flasks. Flasks were incubated for two hours at 37°C before aspirating Gelatin solution.

Cells were passaged at a ratio of 1:6 upon reaching 80% confluence. For passage, cells were released with TrypLE Express Enzyme (12604013, Thermo Fisher Scientific) for one minute in the incubator before adding MV-2 medium to halt enzyme activity and pipetting to make a single cell suspension. Cells were passaged 1:6 by pelleting one sixth of the cell mixture for five minutes at 300 RCF and resuspended in MV-2 medium before being added to a new cell culture dish.

For use in experiments, cells were used upon reaching 80% confluence and harvested as described above.

Cell culture in OrganoPlate

HepG2 cells were harvested as described above, pelleted at 300 rcf, and medium was aspirated. Cells were resuspended in Matrigel® hESC-Qualified Matrix (354277, lot no. 1019001, dilution factor 278 µL, Corning) at a concentration of 1 x 10^6 viable cells/mL. Matrigel was used undiluted, and pipetting steps involving Matrigel were performed on ice to avoid premature polymerization. Cell counting and viability analysis were performed using a TC20 automated cell counter (1450102, Bio-Rad), with a 1:1 ratio of Trypan Blue solution and cell suspension injected into the counting slide chamber (1450003, Bio-Rad).

To fill the OrganoPlate graft chamber with the HepG2 Matrigel suspension, 3 uL of cell suspension was injected into the middle chamber inlet. Correct gel filling of the chamber was confirmed by microscopic observation. The OrganoPlate was incubated for 20 minutes at 37°C to polymerize Matrigel.

After incubation 50 µL of 2% Gelatin solution (G1393, Sigma-Aldrich) was added to the left channel inlet, and 50 µL of DMEM culture medium was added to the middle chamber inlet and observation window. The OrganoPlate was incubated for two hours at 37°C. Gelatin solution was aspirated from the left channel inlet and outlet, and the left channel was washed once using 50 µl MV-2 growth medium in the inlet and outlet wells. HUVEC cells were seeded into the left channel using the passive pumping technique described by Mimetas[22]: medium was aspirated from the left channel inlet followed by addition of 2 µL 1 x 10^7 HUVEC cell suspension.

The plate was incubated on its side for 2 hours in the incubator to allow the cells to settle against the gel in the middle chamber.

After cells had settled, 50 µL of MV-2 medium was added to the left channel inlet and 50 µL complete DMEM was added to the right channel inlet and outlet. The OrganoPlate was placed on an OrganoFlow® S (MI-OFPR-S, Mimetas) rocker in the incubator to allow for bidirectional flow through the medium channels. The rocker was set to incline between -7 and +7 degrees every eight minutes.

Medium was refreshed every other day, and cells were grown for seven days before being used for experiments. Tamoxifen treatment was added by replacing all medium in the left channel with MV-2 growth medium spiked with 1:2000 v/v 20mM Tamoxifen in DMSO, for a final concentration of 10 µM Tamoxifen. Controls were treated with MV-2 growth medium spiked with 1:2000 v/v DMSO.

Directly before starting cell sampling, OrganoPlate chips were washed four times with PBS, with two minutes of incubation on the rocker during each wash step.

Gradient visualisation experiments

A total of 2 µL of Matrigel (8.8 mg/mL; Corning, 356231) was pipetted into the inlet of the middle chamber and incubated at 37°C for 20 minutes to allow polymerization.

Following polymerization, 50 µL of MV-2 medium was added to both the inlets and outlets of the right channel. For the left channel, 50 µL of dye solution prepared in MV-2 medium was added to the inlets and outlets. The plate was then placed on an OrganoFlow rocker set to incline between -7 and +7 degrees every eight minutes and maintained in the incubator. The dye solution consisted of sodium fluorescein (Sigma, F6337) at 10 µg/mL and 155 kDa TRITC-dextran (Sigma, T1287) at 25 µg/mL.

Imaging was performed using the Confocal Micro XLS-C high-content imaging system (Molecular Devices). For quantitative analysis, a rectangular region of interest (ROI) was defined over the middle chamber, and fluorescence intensity was measured along the x-axis across this region.

Sampling capillary production

Sampling capillaries were produced by pulling borosilicate capillaries (GD-1.2, Narishige) using a micropipette puller (p-97, Sutter Instrument). To reach capillary tip sizes around 20 μm in diameter with clean breaks the following settings were used:

Heat	*Pull*	*Velocity*	*Time*	*Pressure*
Ramp + 30	*0*	*120-150*	*200*	*200*

After pulling, capillaries were scored and broken using the Glass-on-Glass technique, where a second capillary was used to score and break off ¼th of the pulled tip's length. Capillary tip size and quality were confirmed by microscope.

Sampling setup

In order to ensure the sampling capillary holder could reach the chip at the bottom of the adapted Organoplate Graft, a micromanipulator was set up in a configuration that allows for a wide range of sampling angles (supplementary figure 1). Sampling capillaries were placed in a capillary holder (IM-H2, Narishige). The capillary holder was kept in place by a pivoting clamp, which in turn was mounted on a ball joint (B9, Narishige), thus allowing the capillary holder to be positioned by either angling the clamp or turning and tilting the ball joint in a wide range of directions. The ball joint was mounted on a 3-axis micromanipulator (MHW-3, Narishige) in an elevated position using a 4-cm bolt.

Sampling method

Before sampling each cell, the microscope was focused on a cell within the sampling window of the Organoplate Graft. The plate was then removed, after which a fresh sampling capillary was inserted into the micromanipulator capillary holder. The micromanipulator, positioned at an angle to ensure it enters the plate in parallel with the column of lowered titerplate walls, was then used to position the capillary tip into focus, ensuring both cell and capillary would be in the same position. The capillary was horizontal enough that the tip could be seen with the microscope and vertical enough that movement was not completely hindered by the walls of the chip. The capillary was then moved directly up using the

micromanipulator, until enough room was made to replace the Organoplate onto the microscope stage. The capillary holder was then moved directly down using the micromanipulator in order to maneuver the capillary tip directly onto the cell of interest. Using a connected syringe, vacuum was added ensuring the selected cell was picked up, at which point the vacuum was immediately removed and capillary was removed from the gel. With imaging, the amount of force applied to the syringe could be adjusted to avoid pushing out air and establishing enough vacuum to capture the cell. During sampling, the capillary could be used to nudge cells away from the cell of interest. Generally, the force applied to the cell through the capillary was greater than the force binding two cells together, so one cell could be easily selected. Microscopic images were made to confirm the cell(s) were cleanly removed. In the event that the images indicated more than one cell was captured, the sample was discarded. Cells were sampled from chips for a maximum of 60 minutes after chips were washed with PBS.
For blank samples, the process used to capture cells was applied to areas not containing cells, in order to sample the gel and medium normally included alongside cell samples.
Due to the size of the capillaries and the pressure applied when sampling, blockage with ECM did not occur, however, cooling the capillaries remained an option. Additionally, while not used in this study, Corning cell recovery solution (354253, Corning) may be used to break down the ECM.
Capillaries containing sampled cells were then placed into dishes on dry ice, to quickly cool down and freeze. These dishes were stored at -80°C until ready for measurements.

In total, cells were collected from 10 individual chips.

Sample preparation for measurements
To prepare for MS measurements ionization solvent consisting of 80% Acetonitrile, 10% DMSO and 0.1% Formic Acid was prepared, supplemented with 100 nM D5-Tamoxifen as an internal standard. To load the capillary, 3 µL of cold ionization solvent was added to the back of each capillary using GelLoader tips (20µL, Eppendorf). Capillaries were then inserted into a capillary holder connected to a syringe, using positive pressure to push the volume out into a 0.5 mL Eppendorf tube.

Eppendorf tubes were shortly centrifuged to form a single droplet of approximately 3µL, which was pipetted up using GelLoader tips (20µl, Eppendorf) and added to the back of a spray capillary (5µm, Humanix, Japan). Tips were shortly centrifuged to concentrate the volume near the tip, at which point spray tips were ready for mass spectrometry. The combination of the ionization solvent and centrifugation dissociated any ECM that may have been sampled with the cell which could be confirmed by the successful spraying of the sample from the nanospray capillary to the MS during measurements.

Mass spectrometry was performed with an Orbitrap Exploris 480 (Thermo Fisher Scientific). For all measurements, the sample was loaded into a 5µm glass capillary (CT-2, Humanix) with a pipette and 20µl gel loader pipette tip (Eppendorf). The capillary was mounted on an offline nano electrospray ionization source (nano-flex source, Thermo Fisher Scientific). The spray was stabilized according to the total ion count variation and spray current before data acquisition. With nESI, a stable spray was proof that no remnants of the ECM were present for the measurement. The acquisition parameters used in the experiment are listed in Supplementary Table 1. Tamoxifen and 4-hydroxy Tamoxifen (4-OHT) MS/MS acquisition parameters are listed in Supplementary Table 2. Cellular measurements were carried out with the addition of a FAIMS Pro Duo interface (Thermo Fisher Scientific) which are explained in detail in the results section. The normalized Tamoxifen abundance was calculated by dividing the Tamoxifen abundance by the abundance of deuterated Tamoxifen.

The raw data from the mass spectrometer was centroided in XCalibur (Thermo Fisher Scientific). The spectra across scans was averaged in XCalibur to yield one intensity per m/z value in each measurement. Peak picking consisted of identifying the Tamoxifen and deuterated Tamoxifen peaks in each measurement and recording the intensity. The intensity of Tamoxifen in each measurement was normalized using the intensity of the deuterated Tamoxifen. To determine the statistical significance of the intensities of Tamoxifen in cells at different locations, ANOVA followed by Tukey HSD posthoc analysis was performed in R. The plots were created using the ggplot2 library.

Results

To establish a vascularized 3D environment for the model, a commercially available organ-on-chip platform was modified (Organoplate Graft, Mimetas) with some modifications to the wall height to allow sampling.

The stock configuration of this platform integrates 64 individual microfluidic chips within a standard 384-well microtiter plate format. Each microfluidic chip comprises three adjacent channels: a central, open-top grafting chamber designed for direct tissue placement, and a perfusion channel on either side of the chamber (Figure 1a). The chip has inlets and outlets for media perfusion and a microscope-compatible glass bottom to facilitate high-resolution imaging. The grafting chamber and perfusion channels are connected via Phaseguides, ridges at the bottom of the microfluidic that act as capillary barriers, allowing patterning of the ECM gel into the ECM chamber (Figure 1c and 1d). The 1mm wide access hole at the top of the graft chamber is used to insert the microneedle into the ECM gel.

To enable single-cell manipulation within the ECM of the graft chamber, the OrganoPlate® Graft was modified (Figure 2) by reducing the height of the titerplate wall of each of the 64 chips grafting chamber (wall between A2-B2). The height of the walls between the chips (wall between B2-C2 in this example) in this column was reduced to a lesser extent, ensuring no overflow of media between chips while still offering more space for sampling. The wall height was reduced such that insertion of a micromanipulator microneedle at a 40-degree angle from vertical would allow targeting the grafting hole area (1 mm wide hole in the center of the chamber) (Figure 2). After this modification it became possible to use a micromanipulator to sample from the graft chamber.

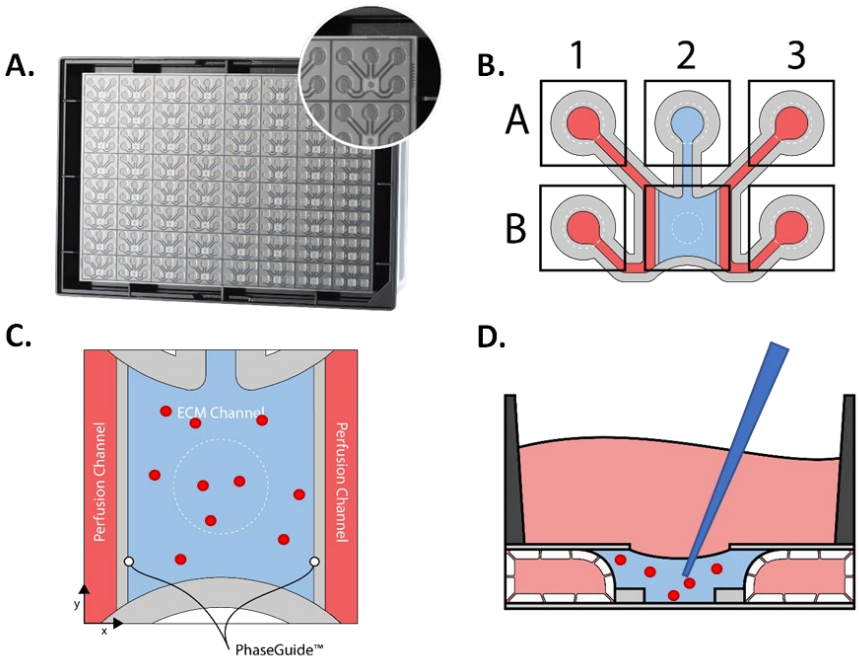

Figure 1 A) A view of the OrganoPlate bottom microfluidics with 64 Grafting chips. B) Layout of an OrganoPlate Graft chip. C) View of the grafting chamber with ECM, media and cells embedded in the ECM. . In the 3D model used for sampling, the left perfusion channel contains HUVEC cells, and is the channel where Tamoxifen-spiked medium is added. D) (not to scale) representation of a microneedle inserted into the ECM through the grafting chamber hole.

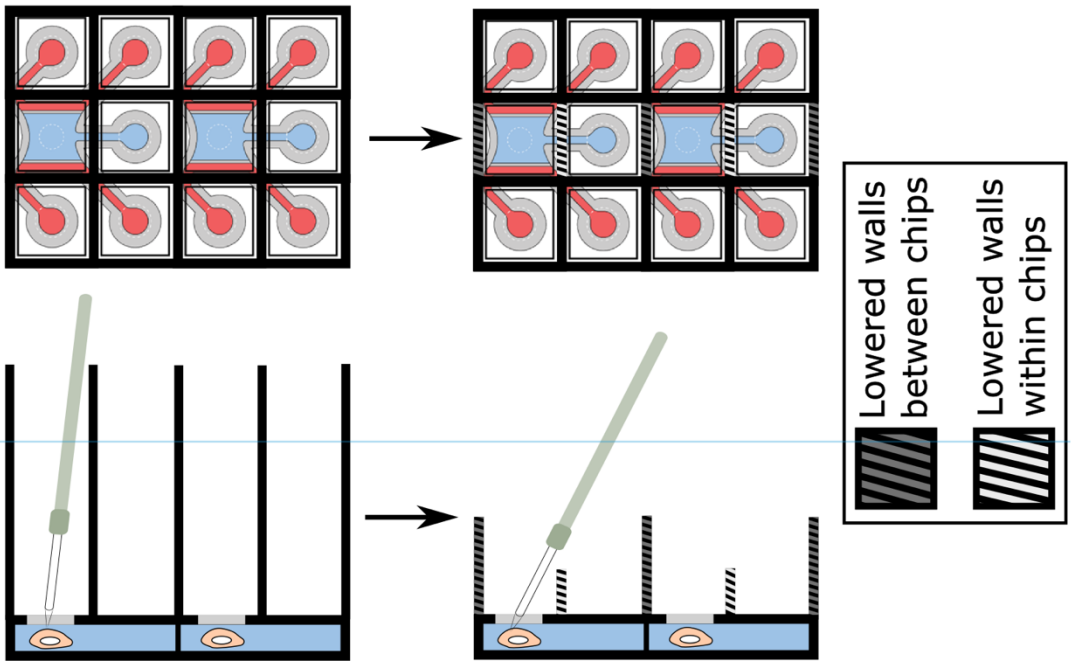

Figure 2. A view of a single Organoplate Graft chip indicating the adaptations to microtiter plate walls used to allow for microneedle sampling. Left chip details the normal state, showing the steep angle required to introduce a needle into the sampling window. Right chip indicates which walls have been lowered to keep separation between chips while allowing a wider range of sampling angles.

To measure the drug heterogeneity in a 3D microenvironment, first, a drug gradient must be established and tested in the organ-on-chip device itself. Then, model establishment and subsequent single-cell sampling from different regions in the microenvironment can commence. Finally, mass spectrometry measurements and data analysis can be used to establish the degree of heterogeneity in the 3D microenvironment in terms of drug uptake and metabolism.

To test if a drug gradient established in the 3D organoplategraft can be used, media spiked with 10 μM of Tamoxifen was infused from one channel (spiked channel), with the other channel infused with media without Tamoxifen (control channel). The experiment was repeated with collagen and Matrigel as the ECM. After 24 hours, samples were measured from both

sides of the channels. Figure 3 shows the abundance of Tamoxifen measured in the spiked and control channels in two different ECM conditions.

To visualize the gradient formation process using fluorescence microscopy, chips loaded with Matrigel were also spiked with 2 different dyes instead of Tamoxifen. Sodium fluorescein was used due to its similar molecular weight to Tamoxifen, while a 155 kDa TRITC-dextran dye was used to study perfusion of larger compounds. After 24 hours, a gradient remained for both dyes used (Supplementary Figures 2,3)

After successfully establishing the gradient, 80 single cells were sampled and analyzed from the established 3D drug spiked HepG2 model. To achieve the highest signal to noise ratio (S/N) possible and ensure Tamoxifen was detected through the noise, FAIMS was employed. FAIMS works by separating ions based on their behavior in electric fields, which are induced and varied with a compensation voltage. This significantly reduces the chemical noise by allowing only select ions to pass into the mass spectrometer. The compensation voltage (CV) was optimized to Tamoxifen and 4-OHT by varying the electric field in increments of 10 over a CV range of -100 to 100 while monitoring the intensity and S/N of the Tamoxifen signal (Supplementary Figure 4). The CV was the only parameter optimized, all other FAIMS parameters were at default settings and are listed in Supplementary Table 3. The compensation voltage alters the electrical field, taking advantage of ion mobility to reduce chemical noise by filtering out unwanted molecules that obscure the signal. The molecule of interest has an ideal mobility to oscillate between the electrodes, while other molecules will come into contact with the electrode and become neutralized. The quality of the measurement was evaluated according to total ion count and signal to noise ratio during and after acquisition. FAIMS measurements showed that it can reduce the noise level to allow for Tamoxifen peak (372.232) detection despite the dilution done to the sample (Figure 4).

Tamoxifen and 4-OHT could be detected and annotated using their accurate mass with an error less than 3 ppm as well as their isotopic C13 peaks. The Tamoxifen peak was further confirmed by its MS/MS fragmentation pattern with a prominent fragment at 129.0685 (Supplementary Figure 5).

Fragmentation patterns were compared to that of previously obtained spectra of standards.

To identify the extent of the heterogeneity of Tamoxifen uptake in the cells, the cells in the 3D model were divided into three groups depending on their position relative to the vasculature providing the drug (close, medium, far). This was done by dividing the graft window into three groups (500-700 μm, 800-1050 μm, and 1100-1450 μm from the spiked channel). Then, the relative abundance of Tamoxifen in individual cells was measured in each group using mass spectrometry. Five blank samples (ionization solvent only), 17 cells from the far section, 21 cells from the center section, and 26 cells from the close section were measured. The maximum Tamoxifen normalized abundance of the channel closest to the Tamoxifen spiked channel is 2.88 which is in contrast to the maximum Tamoxifen normalized abundance of the channel furthest from the Tamoxifen spiked channel, which was 0.61. The results are summarized in Supplementary Table 4. The significance in the difference between locations was established with Tukey's HSD test and is summarized in Supplementary Table 5 and Figure 5.

In an attempt to more accurately correlate the heterogeneity of the cells drug uptake to their respective position in the graft chip and to the drug delivery vasculature, each cell was imaged at the time of sampling recording the exact position of the cell within the chip. (Figure 6, Supplementary Table 6). The abundance of Tamoxifen in each cell relative to its exact position relative to the drug delivery vasculature was then mapped (Figure 7).

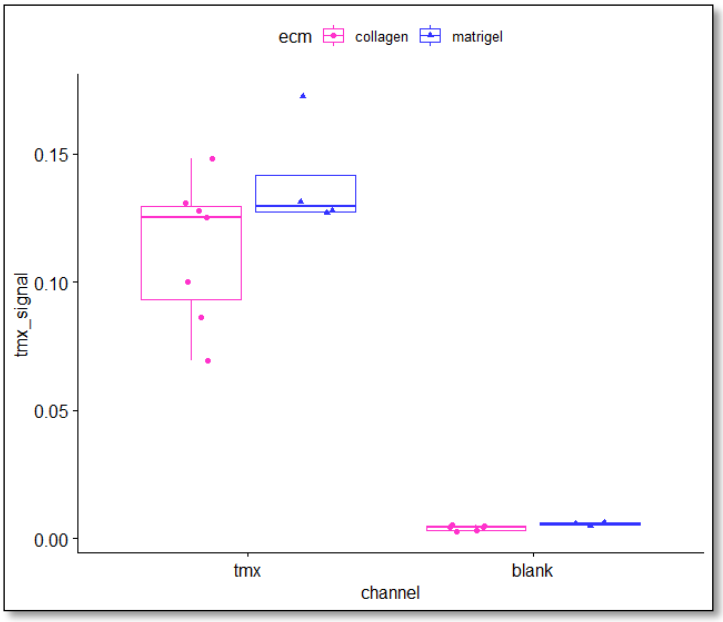

Figure 3: Samples taken from the Tamoxifen spiked channel and the blank media channel indicate that the Tamoxifen does not penetrate into the blank media channel in either Matrigel or Collagen ECM models.

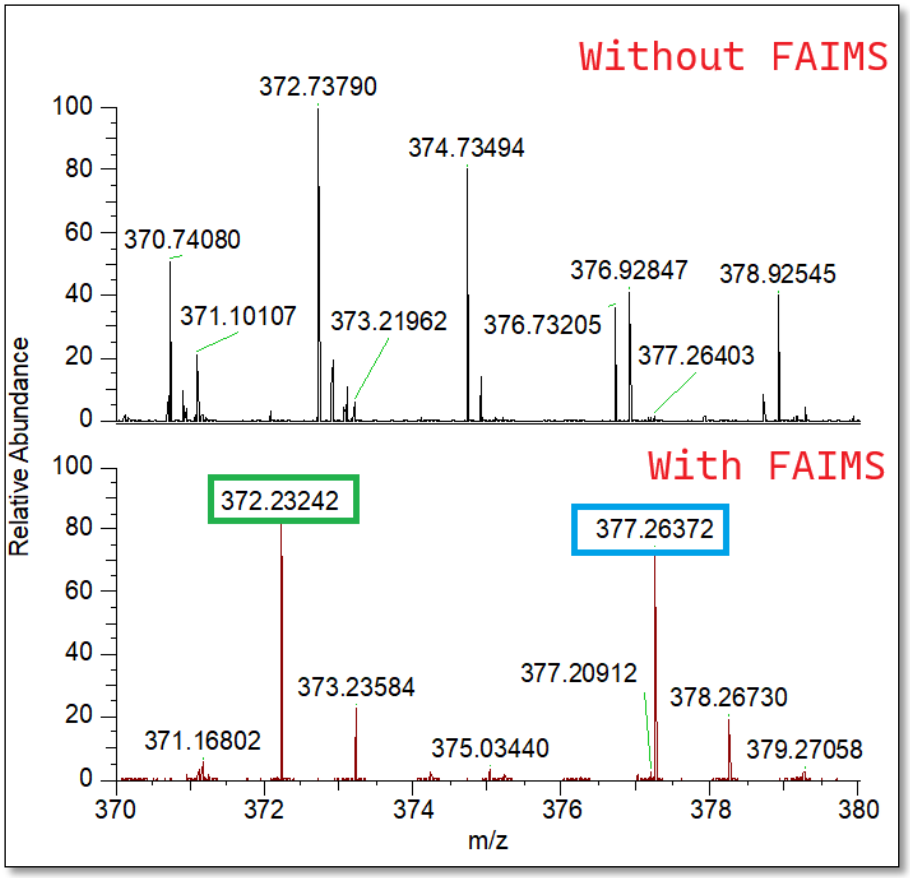

Figure 4: Top: Spectrum of cell lysate measured without FAIMS, targeting Tamoxifen at *m/z* 372.232 and 4-OHT at *m/z* 377.264 (no peaks visible). Bottom: Spectrum of cell lysate measured with FAIMS, compensation voltage of -30 V, targeting Tamoxifen at *m/z* 372.232 (boxed in green) and 4-OHT at *m/z* 377.264 (boxed in blue). The spectra are normalized to each other such that the relative abundances are comparable across both spectra.

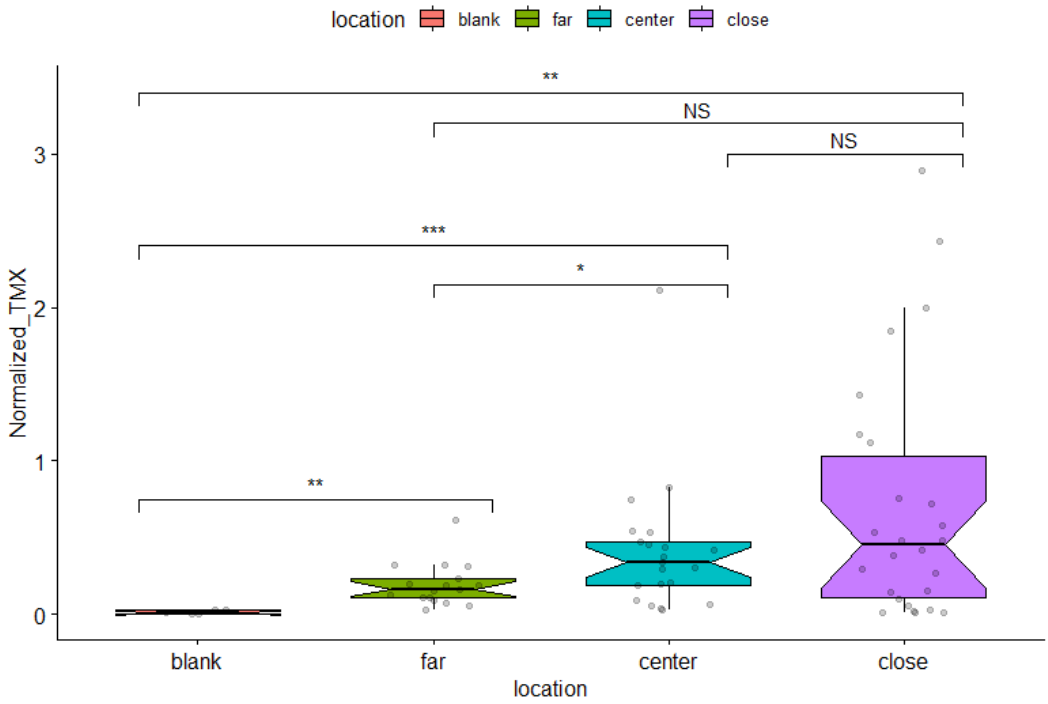

Figure 5: Distribution of normalized Tamoxifen at categorically defined locations with respect to the spiked Tamoxifen channel.

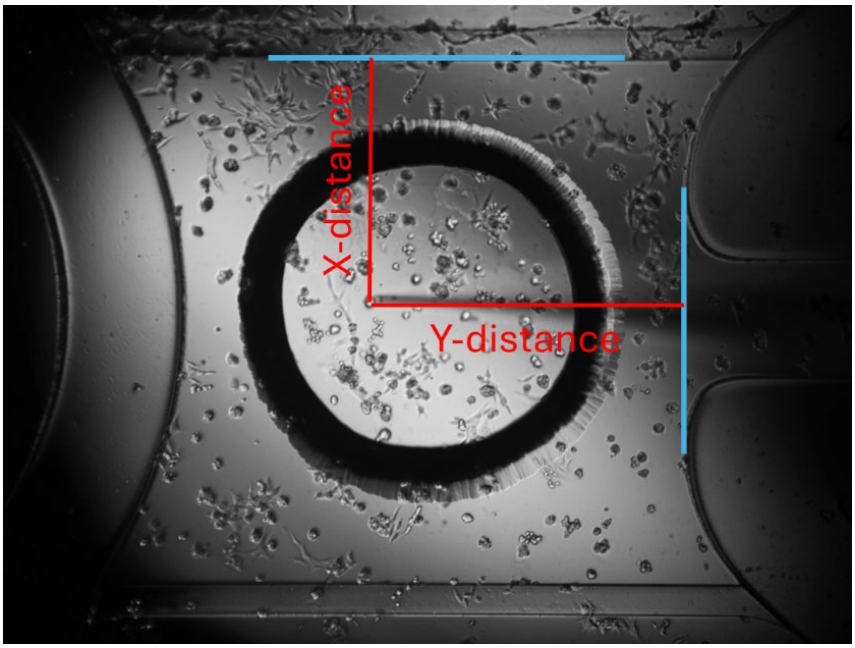

Figure 6: Each cell is imaged at time of sampling, recording the exact location in the chip with respect to the various channels.

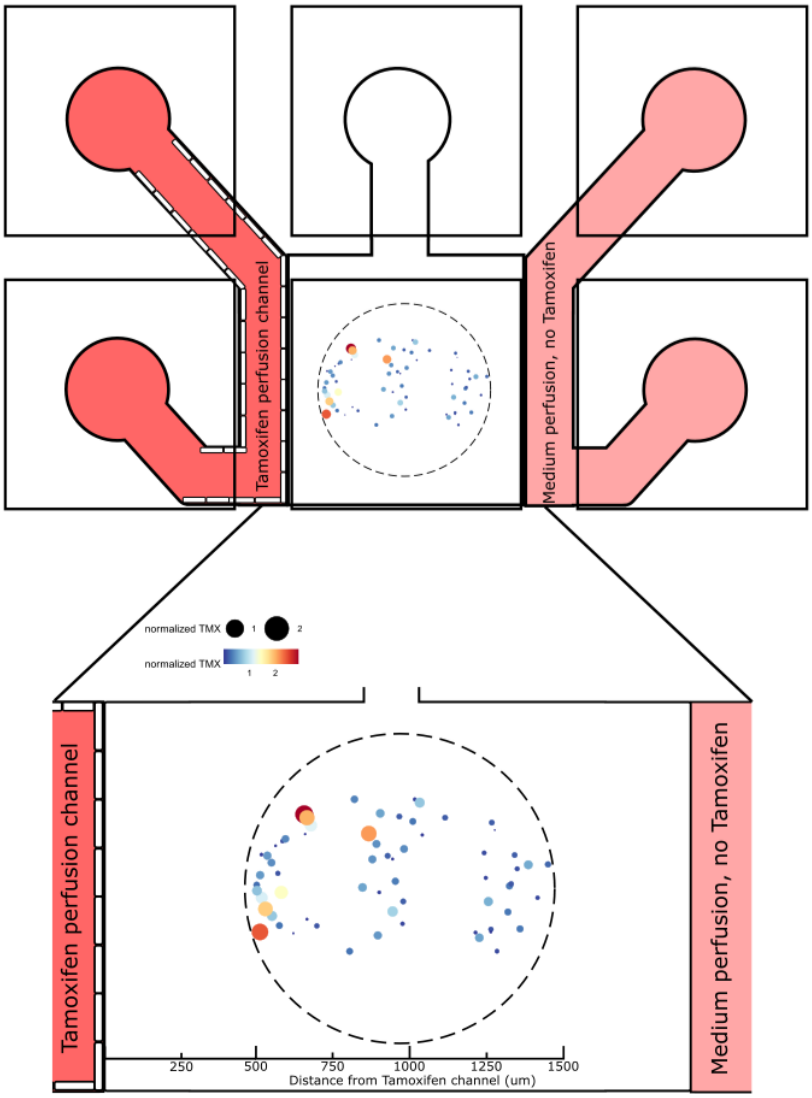

Figure 7: Overview of sampling locations of individual cells in an Organoplate Graft chip. Indicated in the highlighted area are the observation window of the Organoplate Graft, and the cells sampled from the 1mm sampling window. Cell sampling locations are plotted to scale according to the measured x-and y-distances. The points are colored by a gradient and scaled in size to indicate the normalized Tamoxifen intensity.

Discussion

In this study we have established an organ-on-chip model capable of establishing a drug gradient and then built an analytical pipeline that enables mapping out the heterogenous behavior of individual cells in the 3D

model. The two main limitations in capillary microsampling in 3D environments (geometry and ECM interference) were circumvented by modifying the organ-on-chip plate, adding an extra sample preparation step, followed by FAIMS usage to improve the signal. The abundance of Tamoxifen was measured in single-cells obtained from the vascularized 3D model and the degree of heterogeneity was calculated. Furthermore, the correlation between the relative position of the cells to the drug-spiked vessel and Tamoxifen abundance was studied as well. Thus, showing the extent of drug uptake heterogeneity in cancer cells as well as the drug's spatial distribution the tumor microenvironment.

Gradients play a pivotal role in various biological processes such as chemotaxis, embryonic development, and angiogenic processes.[23] Studies have shown that some enzyme responses and pathway activation is dependent on the concentration of an activator, which creates concentration heterogeneity among cells.[24] An additional level of heterogeneity is introduced in drug uptake even in uniform environments.[25] In situations in which a drug gradient exists, the cellular uptake heterogeneity is compounded with the heterogeneity of drug availability and possibly, the cell position. By exposing cells to compound gradients, our approach could enable investigation of concentration-dependent cellular responses, which are often observed in vivo but challenging to investigate in traditional in vitro models. Our results show we can measure heterogeneity in drug uptake in the case of HepG2 cells exposed to a Tamoxifen gradient (Figure 5). This understudied drug uptake heterogeneity poses a significant challenge in drug efficacy modeling.[29] There are multiple likely reasons for this heterogeneity such as differences in the expression of efflux transporters, and varying rates of intracellular metabolism and compartmentation of the drug. These cellular differences result in a large variation of the drug's effective concentration, necessitating single-cell analytical methods to assess drug response on the cellular level.

Heterogeneity in 3D systems have been shown in the case of cellular uptake of nanoparticles in previous studies[30]. Similarly, heterogenous uptake of several chemotherapeutic agents was studied in A549 cell spheroids using stimulated Raman scattering microscopy[31], as was heterogenous uptake of a

fluorescently labeled PARP inhibitor using *in vivo* imaging[32]. Therefore, we would expect to see similar variation in the uptake of Tamoxifen across the gradient following probability distribution functions. Our data, summarized in Supplementary Table 4, show a higher measured abundance of Tamoxifen in the cells near the Tamoxifen spiked channel, in contrast to the abundance of Tamoxifen in cells farthest from the Tamoxifen spiked channel. However, the intensity of Tamoxifen did not closely reflect the expected gradient, indicating heterogeneity in drug uptake in individual cells.

Matrigel is a complex matrix consisting of thousands of proteins that influence the metabolic pathways, which makes it crucial to cell models, however, it can hinder the mass spectrometry scans of the cells.[33] To ensure optimal measurements of the cells, the Matrigel should be removed from the cells prior to measuring with one of several methods.[33] In experiments that specifically aim to analyze the ECM, the Matrigel is prepared by washing with a solution containing ammonium bicarbonate to elute the components of interest as even in these cases the Matrigel is not measured as it is with the cells.[34] The Matrigel is one of the reasons that the standard single cell sampling method must be amended in this study. By adding sample preparation between sampling and direct injection, the robustness of the measurement is preserved.

A significant level of chemical noise is generated with direct injection mass spectrometry, especially with high resolution mass spectrometers.[35] In this study, the Tamoxifen target could not be evaluated through the noise. Previous studies implemented FAIMS in proteomics workflows to reduce the noise and ultimately identify heterogeneity in single cells.[36] The application of FAIMS for single cell metabolomics has not been reported, however, Figure 4 shows a clear improvement in the detection of Tamoxifen when FAIMS was used. For this study, FAIMS was optimized for the Tamoxifen target with variation of the compensation voltage (Supplementary Figure 4). There are two main contributors to the successful implementation of FAIMS for single cell metabolomics, injecting a cell lysate and having a targeted workflow. Injecting an intact cell hinders the establishment of a stable spray and an untargeted workflow complicates the optimization of the compensation voltage.

There were several limitations in this study, including the throughput, availability of a suitable chip, and the 3D model itself. Sampling throughput could be improved by utilizing robotic sampling instead of the described manual sampling method. Sample transfer using microfluidics, or segmented flow would also aid in increasing sample throughput by eliminating the need to backfill each capillary and centrifuge individually. These approaches have the additional advantage of reducing sample transfer steps, and consequently, sample loss. Aside from the throughput considerations, automating the sampling allows for vertical sampling, improving compatibility with different organ-on-chip platforms. Finally, in order to best accommodate single cell sampling, the density of the cells was lower than generally used in biological studies. The aim of the study was to validate our platform, so the model was designed relatively simply, with one cell line and low cell density. To further validate the results of this study and to increase the biological relevance, the experiment should be repeated with more complex samples, including increased density of cells, other cell lines, and co-cultures integrating organoids. Despite the aforementioned limitations, this technology, in its current state can already be applied to several unanswered biological questions such as investigating angiogenesis and developing vascularized tissue models in vitro [38], investigating molecular mechanisms governing chemotaxis in the tumor microenvironment, as well as the interaction of tumor cells with the host microenvironment.

Conclusion

In this study, we aimed to show that an OrganoPlate microfluidic chip could be used to establish a drug gradient and that exposed cells could be individually captured directly from the chip, through Matrigel, and measured to analyze the drug uptake. We successfully modified the chip to account for the limitations of single cell sampling and through various steps established that a gradient exists between the media channels of the chip and cells could be directly sampled. Mass spectrometry allowed us to measure the abundance of Tamoxifen in all cells exposed to the gradient. While there

were several limitations in this study, we established the validity of this technique.

Future perspectives include the use of this method in more clinically relevant 3D models, sampling from 3D cell cultures with higher cell densities and multiple cell types. Additionally, further development of this technique includes the use of robotic sampling approaches to improve sampling speed, and utilizing microfluidics and segmented flow approaches to reduce handling steps and sample loss. Together, these approaches would increase sample throughput, leading to more samples and thus higher statistical robustness of the data gathered from each sampled chip.**Data availability**

The data that supports the findings of this study are available from the corresponding author upon request.

References

1. Fontoura, J. C. *et al.* Comparison of 2D and 3D cell culture models for cell growth, gene expression and drug resistance. *Mater. Sci. Eng. C* **107**, 110264 (2020).
2. Duval, K. *et al.* Modeling Physiological Events in 2D vs. 3D Cell Culture. *Physiology* **32**, 266–277 (2017).
3. Du, Y. *et al.* Synthetic sandwich culture of 3D hepatocyte monolayer. *Biomaterials* **29**, 290–301 (2008).
4. Vinci, M. *et al.* Advances in establishment and analysis of three-dimensional tumor spheroid-based functional assays for target validation and drug evaluation. *BMC Biol.* **10**, 29 (2012).
5. Lancaster, M. A. & Knoblich, J. A. Organogenesis in a dish: Modeling development and disease using organoid technologies. *Science* **345**, 1247125 (2014).
6. Zervantonakis, I. K., Kothapalli, C. R., Chung, S., Sudo, R. & Kamm, R. D. Microfluidic devices for studying heterotypic cell-cell interactions and tissue specimen cultures under controlled microenvironments. *Biomicrofluidics* **5**, 013406 (2011).
7. Lee, M.-C. W. *et al.* Single-cell analyses of transcriptional heterogeneity during drug tolerance transition in cancer cells by RNA sequencing. *Proc. Natl. Acad. Sci.* **111**, (2014).
8. Ghasemi, M., Turnbull, T., Sebastian, S. & Kempson, I. The MTT Assay: Utility, Limitations, Pitfalls, and Interpretation in Bulk and Single-Cell Analysis. *Int. J. Mol. Sci.* **22**, 12827 (2021).
9. Schnell, U., Dijk, F., Sjollema, K. A. & Giepmans, B. N. G. Immunolabeling artifacts and the need for live-cell imaging. *Nat. Methods* **9**, 152–158 (2012).
10. Cazaux, M. *et al.* Single-cell imaging of CAR T cell activity in vivo reveals extensive functional and anatomical heterogeneity. *J. Exp. Med.* **216**, 1038–1049 (2019).

11. Lentz, C. S. What you see is what you get: activity-based probes in single-cell analysis of enzymatic activities. *Biol. Chem.* **401**, 233–248 (2020).
12. Gebhardt, J. C. M. *et al.* Single-molecule imaging of transcription factor binding to DNA in live mammalian cells. *Nat. Methods* **10**, 421–426 (2013).
13. Elf, J., Li, G.-W. & Xie, X. S. Probing Transcription Factor Dynamics at the Single-Molecule Level in a Living Cell. *Science* **316**, 1191–1194 (2007).
14. Wu, A. R. *et al.* Quantitative assessment of single-cell RNA-sequencing methods. *Nat. Methods* **11**, 41–46 (2014).
15. Anderson, N. M. & Simon, M. C. The tumor microenvironment. *Curr. Biol.* **30**, R921–R925 (2020).
16. Charwat, V. *et al.* Potential and limitations of microscopy and Raman spectroscopy for live-cell analysis of 3D cell cultures. *J. Biotechnol.* **205**, 70–81 (2015).
17. Fujii, T. *et al.* Direct metabolomics for plant cells by live single-cell mass spectrometry. *Nat. Protoc.* **10**, 1445–1456 (2015).
18. Ali, A. *et al.* Single-Cell Screening of Tamoxifen Abundance and Effect Using Mass Spectrometry and Raman-Spectroscopy. *Anal. Chem.* **91**, 2710–2718 (2019).
19. Zhu, Y., Liu, R. & Yang, Z. Redesigning the T-probe for mass spectrometry analysis of online lysis of non-adherent single cells. *Anal. Chim. Acta* **1084**, 53–59 (2019).
20. McMahon, W. P., Dalvi, R., Lesniewski, J. E., Hall, Z. Y. & Jorabchi, K. Pulsed Nano-ESI: Application in Ion Mobility-MS and Insights into Spray Dynamics. *J. Am. Soc. Mass Spectrom.* **31**, 488–497 (2020).
21. Tabassum, H., Rehman, H., Banerjee, B. D., Raisuddin, S. & Parvez, S. Attenuation of tamoxifen-induced hepatotoxicity by taurine in mice. *Clin. Chim. Acta* **370**, 129–136 (2006).
22. Van Duinen, V. *et al.* Standardized and Scalable Assay to Study Perfused 3D Angiogenic Sprouting of iPSC-derived Endothelial Cells In Vitro. *J. Vis. Exp.* 59678 (2019) doi:10.3791/59678.
23. Kim, S., Kim, H. J. & Jeon, N. L. Biological applications of microfluidic gradient devices. *Integr. Biol.* **2**, 584 (2010).
24. Huang, X. P., Da Silva, C., Fan, X. T. & Castagna, M. Characteristics of arachidonic-acid-mediated brain protein kinase C activation: evidence for concentration-dependent heterogeneity. *Biochim. Biophys. Acta BBA - Mol. Cell Res.* **1175**, 351–356 (1993).
25. Deng, B. *et al.* Quantitative study of cellular heterogeneity in doxorubicin uptake and its pharmacological effect on cancer cells. *Biomed. Chromatogr.* **28**, 1393–1401 (2014).
26. Guo, X. *et al.* Creating 3D Angiogenic Growth Factor Gradients in Fibrous Constructs to Guide Fast Angiogenesis. *Biomacromolecules* **13**, 3262–3271 (2012).
27. Ashe, H. L. & Briscoe, J. The interpretation of morphogen gradients. *Development* **133**, 385–394 (2006).
28. Donà, E. *et al.* Directional tissue migration through a self-generated chemokine gradient. *Nature* **503**, 285–289 (2013).
29. (2019).

Supplementary

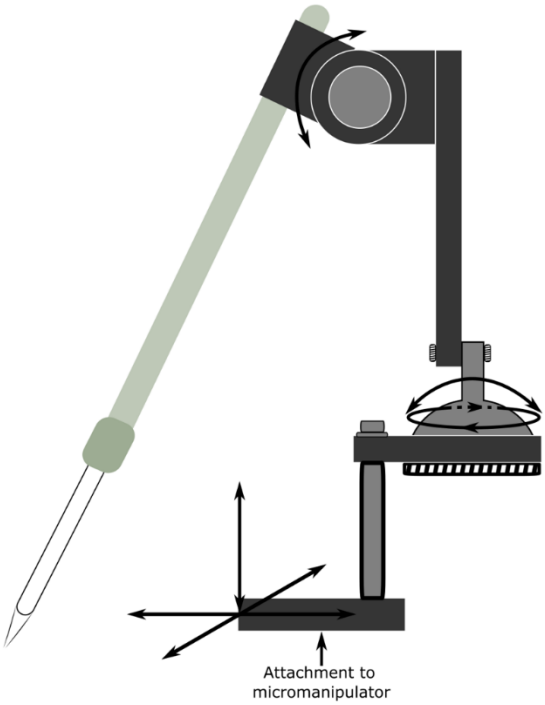

Supplementary Figure 1: a schematic overview of attachments used with the micromanipulator for sampling from the Organoplate. Indicated are parts which provide movement, including the micromanipulator itself, a ball joint and a pivoting capillary holder clamp. Dimensions are not to scale.

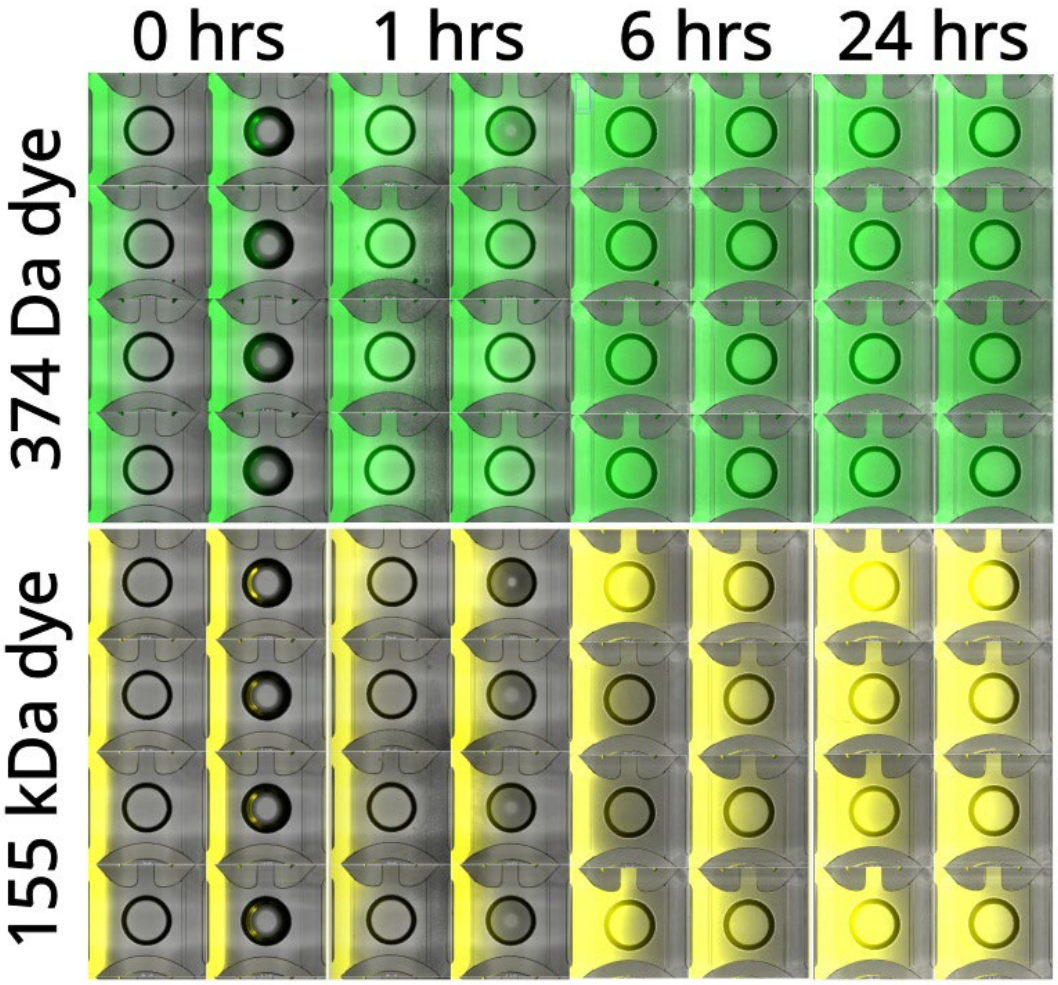

Supplementary Figure 2: Visualization of gradient formation in Organoplate Graft. Dye distribution over the chip was imaged at indicated incubation times. Indicated in green is the 374 Da sodium fluorescein dye, indicated in yellow is the 155 kDa TRITC-dextran dye.

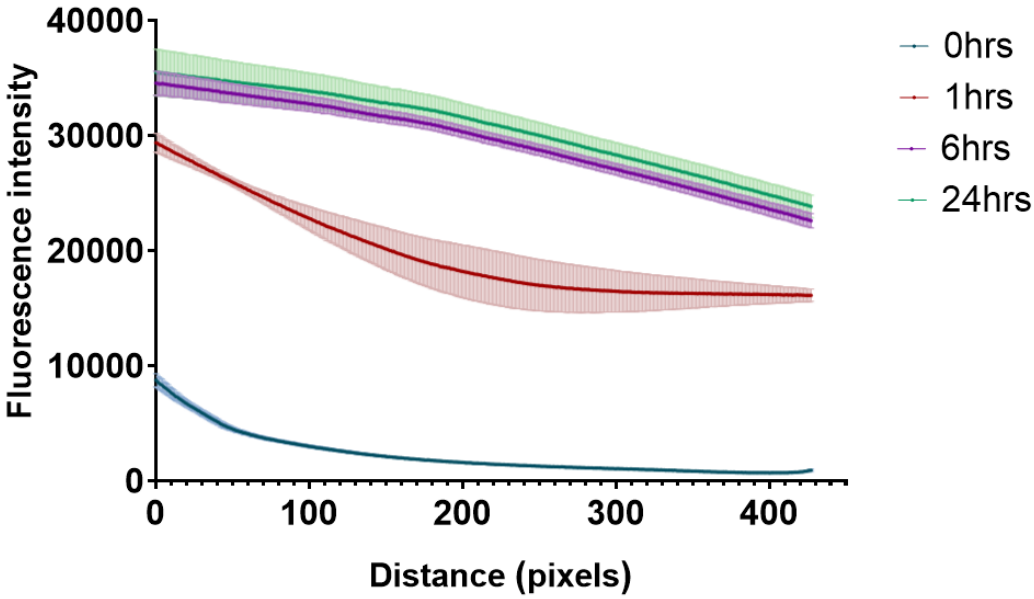

Supplementary Figure 3: quantified fluorescence signal of 374 Da sodium fluorescein dye over Organoplate Graft chip. Distance in pixels represents average signal over the x axis of an Organoplate Graft chip central chamber, with a distance of 0 pixels representing the left side of the central chamber, and 427 pixels the right side of the central chamber.

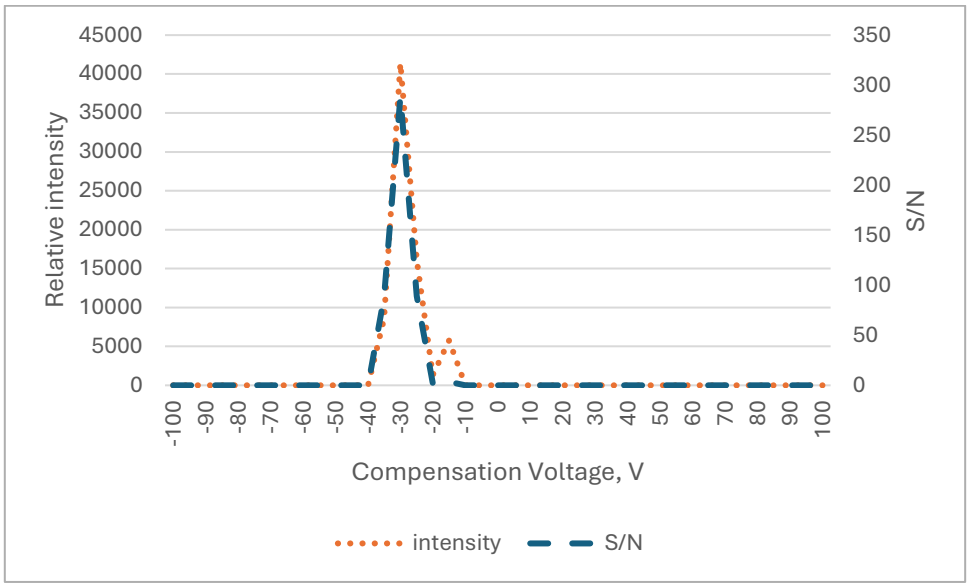

Supplementary Figure 4: Relative intensity and signal to noise ratio (S/N) of the Tamoxifen peak (*m*/*z* 372.23) at various compensation voltages.

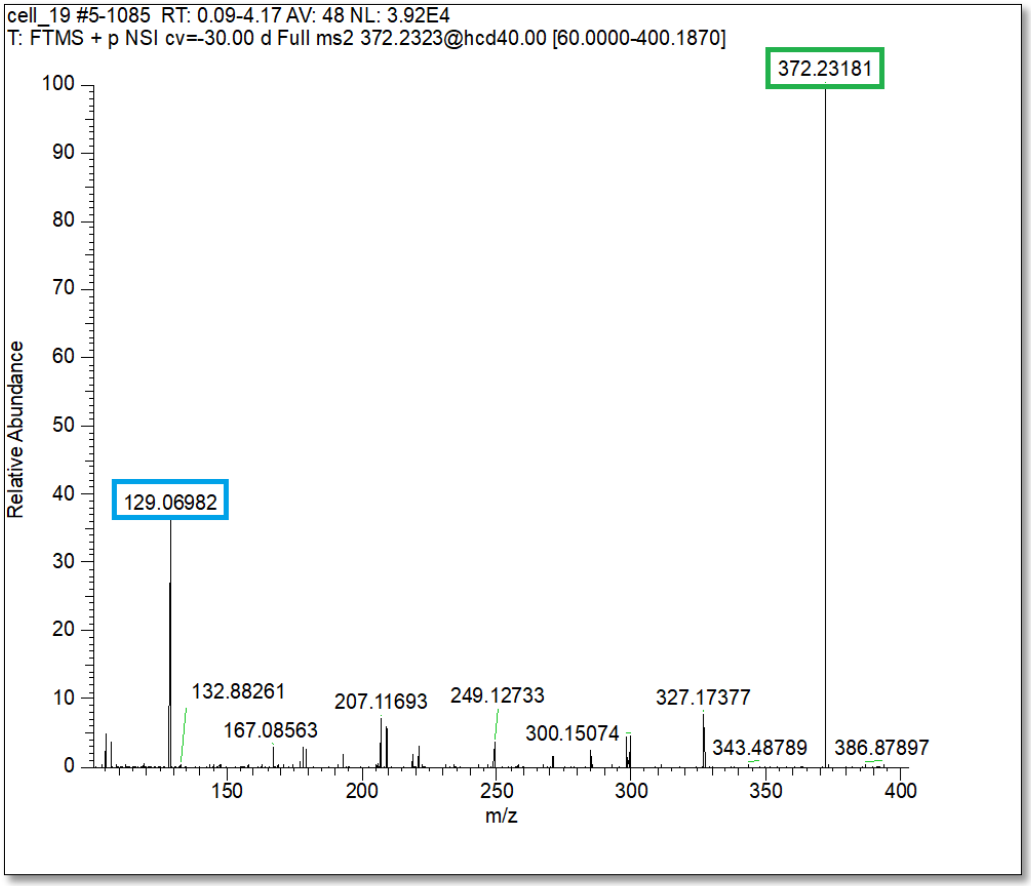

Supplementary Figure 5: Tamoxifen has a known fragmentation pattern with a peak at 129.069, which is used to confirm the peak at 372.232 is Tamoxifen.

Supplementary Table 1: MS acquisition parameters

Parameter	Value
Voltages, positive mode	1700 V
Voltages, negative mode	1000 V
Ion tube temperature	300°C
RF lens	50%
AGC target	Standard
Maximum Injection time	Auto
Mass range	100-800; 350-400
Total acquisition time	8 minutes
Orbitrap resolution	120000

Supplementary Table 2: MS2 parameters

Parameter	Value
Isolation window	1 (m/z)
HCD collision energy	40%
Orbitrap resolution	15000

Supplementary Table 3: FAIMS parameters

Parameter	Value
Compensation voltage	-30
Carrier gas flow	4.6
FAIMS mode	Standard resolution

Supplementary Table 4: Tamoxifen measurement summary

	Minimum	Maximum	Standard Deviation
Blank	0.0000	0.0269	0.0132
Far	0.0247	0.6121	0.1411
Center	0.0263	2.1148	0.4497
Close	0.0094	2.8865	0.8022

Supplementary Table 5: Tukey HSD

Location Comparison	Tukey HSD p-adjusted value
Blank – Far	0.9203
Blank – Center	0.4748
Blank – Close	0.0644
Close – Far	0.0237
Close – Center	0.3028
Center – Far	0.6181

Supplementary Table 6: cell positions

Sample	X distance	Y distance	Time until sampling (minutes after wash)
cell 12	574.514	991.000	5
cell 13	1409.978	872.062	13
cell 14	700	734.834	25
cell 15	1238.095	1090.909	36
cell 16	965.368	1268.398	45
cell 17	980.562	1110.227	59
cell 18	554.113	1043.299	6
cell 19	522.678	872.570	13
cell 21	1112.583	1262.696	25
cell 22	1243.363	969.027	33
cell 23	977.873	854.028	37
cell 25	662.366	1182.796	53
cell 26	1015.119	1352.052	59
cell 28	589.52	1148.474	4
cell 29	624.454	698.691	10
cell 30	668.103	767.243	23
cell 31	820.96	1352.695	28
cell 32	805.43	610.860	36
cell 33	900.648	898.488	42
cell 34	1319.57	929.596	47
cell 35	1325.167	939.866	52
cell 36	1344.444	1013.375	59
cell 37	517.094	705.141	7
cell 38	680.942	1224.850	12
cell 39	540.773	1077.390	17
cell 40	952.586	952.598	25
cell 41	943.723	805.195	33
cell 42	896.104	688.325	38
cell 43	1314.534	802.605	43
cell 44	1353.579	720.188	48
cell 45	1336.226	1080.341	55

cell 46	659.341	1279.154	6
cell 47	555.799	783.370	10
cell 48	517.544	982.468	15
cell 49	927.79	1076.595	23
cell 50	847.007	922.405	29
cell 51	975.61	745.130	35
cell 53	1380.22	1032.979	50
cell 54	1272.331	1202.646	55
cell 55	1222.707	676.914	60
cell 56	599.128	1159.493	4
cell 57	567.1	1125.541	8
cell 58	585.683	898.060	16
cell 59	878.587	1059.605	21
cell 60	891.832	1134.660	27
cell 61	1030.973	1336.291	32
cell 62	1262.814	1238.822	37
cell 63	1210.469	702.304	45
cell 64	1260.065	718.149	52
cell 65	1259.636	705.012	59
cell 66	521.739	1082.609	5
cell 67	534.783	817.391	10
cell 68	668.113	1262.505	15
cell 69	943.478	1060.905	21
cell 70	1039.13	1178.333	27
cell 71	867.102	1185.185	32
cell 72	1251.641	853.392	36
cell 73	1279.476	611.355	40
cell 74	1443.478	1034.792	45
cell 75	506.55	934.510	6
cell 76	579.521	736.396	10
cell 77	507.592	906.726	14
cell 78	903.93	1283.912	19
cell 79	1008.734	1244.552	24